Melting in small gold clusters: a density functional molecular dynamics study

2006 J. Phys.: Condens. Matter 18 55

(http://iopscience.iop.org/0953-8984/18/1/004)

INSTITUTE OF PHYSICS PUBLISHING JOURNAL OF PHYSICS: CONDENSED MATTER

J. Phys.: Condens. Matter **18** (2006) 55–74 doi:10.1088/0953-8984/18/1/004

Melting in small gold clusters: a density functional molecular dynamics study

B Soulé de Bas, M J Ford[1] and M B Cortie

Institute for Nanoscale Technology, University of Technology, Sydney, PO Box 123, Broadway, NSW 2007, Australia

E-mail: mike.ford@uts.edu.au

Received 19 August 2005
Published 9 December 2005
Online at stacks.iop.org/JPhysCM/18/55

Abstract

Molecular dynamics simulations of the thermal behaviour of gold clusters containing 7, 13 and 20 atoms have been performed. Total energies and forces at each step of the simulation are calculated from first principles using density functional theory. Ion trajectories are then calculated classically from these forces. In each case the global minimum energy structure and a low-lying isomer are used as the starting structures. In most cases, the clusters do not exhibit a sharp transition from a solid-like phase to a liquid-like phase, but rather pass through a region of transformations between structural isomers that extends over a considerable temperature range. Solid-like behaviour is observed in the atomic trajectories of the simulation at temperatures up to, or above, the bulk melting point. The 20-atom tetrahedral structure is the one exception, showing a sharp transition between solid-like and liquid-like phases at about 1200 K. The starting structure used in the simulation is shown to have a considerable effect upon the subsequent thermal behaviour.

1. Introduction

The manner in which phase changes such as melting and freezing apply to small clusters of atoms is an interesting question, and there have been a number of computational and experimental studies of these phenomena to determine the temperatures at which the transitions between solid-like and liquid-like structures occur [1–11]. The intuitive result that melting temperature decreases with cluster size is often quoted [1, 12–16]. This behaviour can be understood in terms of the proportion of surface to bulk atoms in the cluster as a function of size. However, while this trend is well established for clusters containing thousands of atoms, this is not true for very small clusters, with tens of atoms. This has been shown by

[1] Author to whom any correspondence should be addressed.

the experimental studies by Shvartsburg and Jarrold [4] and Breaux *et al* [5] on Sn and Ga nanoparticles, respectively.

Metallic clusters in this size range are definitely not bulk-like, and even the concept of bulk and surface atoms is lost. Neither are they molecules in the sense that there is directional bonding. The concepts of melting and phase transitions or vibrational modes and bond dissociation are difficult to apply. Berry [17] has already tackled this problem at a fundamental level and drawn an important connection between thermal behaviour and the shape of the potential energy surface (PES). The conclusion of this work is that clusters do not generally show well-defined melting and freezing unless the potential energy surfaces contain distinct, separated regions of liquid-like and solid-like behaviour. In many cases the cluster exists in a slush-like state with varying proportions of solid-like and liquid-like properties over a range of temperatures.

Most of the current understanding of the microscopic behaviour of clusters at finite temperatures has been gained by simulation using a variety of molecular dynamics (MD) methods [6, 7, 9, 10, 18]. Experimental studies to determine these properties directly are obviously very demanding and, despite a number of important discoveries made [2, 4, 5], a definitive picture is yet to emerge. In most of the simulations the microscopic structure is characterized in terms of bond-lengths and their average fluctuations over many cycles of the MD simulation [19–21]. Melting of the cluster where atoms go from vibrating about a mean position to translation within the cluster is then accompanied by a sharp increase in the bond fluctuation. Consistent with the accepted view of melting in bulk materials, discontinuities have also been observed in the energy versus temperature curves for clusters [16, 19–21]. In addition to these phenomenological studies, MD simulations have also been analysed following a more thermodynamically oriented technique, termed the multiple-histogram (MH) [22, 23], which leads to the determination of the entropy and the specific heat of the system. However, in most MD investigations, little or no emphasis is placed upon the shape of the PES and its effect upon melting dynamics. This is surprising given that molecular dynamics is a computational tool for exploring the PES in an efficient manner. For metallic clusters it is also an important consideration given that the PES can be extremely complex with a large number of shallow minima.

In our previous study [24] we have explored the PES of gold clusters in the size range 3–38 atoms using static techniques, that is, by single-point energy calculations or geometry optimizations to minima. A combination of empirical potentials and density functional calculations were used to identify global minimum energy structures. Gold clusters are of particular interest due to their surprising catalytic activity [25, 26]. It is important to know whether they present to the environment with a solid-like or liquid-like structure at a given temperature since that might have an influence on their efficacy. In the present paper we extend our previous work to *ab initio* MD studies of the thermal stability of these small clusters. The aim is to assess whether gold clusters in this size range have well-defined melting points and, if so, how they vary with size. In addition to the ground-state structures determined previously, the melting of structural isomers is studied to determine the importance of the initial structure on the thermal stability. By comparison we can relate the thermodynamic behaviour observed in the present MD simulations to the features observed in the PES in our previous study.

We focus our attention on three sizes: $n = 7$, 13 and 20. The $n = 7$ cluster corresponds to the planar to three-dimensional (3D) transition at the level of theory used in the present study. The pentagonal bipyramid was therefore studied together with the more stable planar structure reported in [24]: the one-atom capped triangle structure. The Au_{20} cluster is particularly interesting as it has an unexpected, and extremely stable, tetrahedral structure as first reported by Wang and co-workers [27]. As well as studying this structure, we also examined the

thermal behaviour of the disordered Au_{20} second lowest energy structure found in [24], whose geometry is similar to the Au_{19} and Au_{21} global minima [24]. The size $n = 13$ was finally chosen because it corresponds to the size midway between Au_7 and Au_{20}. MD simulations were performed on both the disordered ground-state structure [24] and the 'magic number' 13-atom icosahedron.

2. Methods

Three series of same-temperature isothermal MD simulations were carried out on each of the six structures discussed above with temperature, T, varying from 100 to 2200 K. The MD simulations were performed within the density functional theory (DFT) framework as implemented in the SIESTA code [28, 29]. While the electrons are treated at the *ab initio* level by solving the Kohn–Sham equations self-consistently, the ionic trajectories are generated classically in the canonical ensemble according to the method proposed by Nosé [30]. In this scheme, the system is connected to a thermal reservoir that allows energy to flow dynamically from the reservoir and back so that the mean temperature of the system is kept constant. The strength of the coupling (and therefore the rate at which the instantaneous temperature fluctuates) is controlled by a thermal inertia parameter Q [30]. This MD procedure is implemented into SIESTA with a predictor–corrector type of algorithm that generates the ionic trajectories based upon the knowledge of the atomic positions and forces at each time step.

The DFT calculations were carried out in the local spin density approximation (LSDA) as parameterized by Perdew and Zunger [31]. The atomic forces and stresses were calculated quantum mechanically using the Hellman–Feymann theorem (including Pulay corrections) [29]. Relativistic effects that are known to be important in the quantum chemistry of gold [32–35] were included in the relativistic Troullier–Martins norm-conserving pseudo-potential [36] describing the core electrons. The cut-off radii (r_c) of the pseudo-potential were set to 2.24, 2.24, 2.32 and 1.48 bohr for the s, p, d and f orbitals, respectively. The 5d and 6s valence electrons were represented with a double-zeta basis set with d-orbital polarization. The atomic orbitals were spatially confined by applying an energy shift of 0.02 Ryd [29, 37]. The equivalent plane-wave energy cut-off was set to 100 Ryd. We have previously verified that these parameters represent well-converged values [24] and reproduce bulk gold and gold dimer properties well.

The MD simulations were performed with a time step $\mathrm{d}t = 2.5 \times 10^{-15}$ s and a thermal inertia parameter $Q = 50$ Ryd fs^2. The simulation time step, which corresponds to 1/60th of the highest vibrational frequency of the Au_{20} tetrahedron ($\omega = 221$ cm^{-1}), conserves, to an acceptable degree, the total energy of the extended system, i.e. the total energy of the cluster plus the total energy of the thermal reservoir to which it is connected [30]. The thermal inertia parameter is low enough to prevent large temperature fluctuations (more consistent with constant energy simulations) but high enough to allow the system to equilibrate.

Atomic binding energies and vibrational frequencies of the ground-state structures were determined in order to gain a better understanding of the structural mechanisms occurring in the simulations. The binding energy E_b of a given atom within a cluster was computed as

$$E_b = E_{Cl} - (E_{At/Ghost(Cl-At)} + E_{Cl-At/Ghost(At)}) \quad (1)$$

where E_{Cl} is the total energy of the cluster, and $E_{At/Ghost(Cl-At)}$ and $E_{Cl-At/Ghost(At)}$ are the energies of the separated components taking into account basis set superposition error using the standard counterpoise correction technique [38]. The vibrational frequencies of the clusters were obtained with the VIBRA program [29], which extracts the Hessian matrix from the

atomic force calculations carried out beforehand with SIESTA. These calculations, referred to as force constant (FC) calculations in SIESTA [37], yield atomic forces in response to infinitesimal atomic displacements in the x, y and z directions

Each isothermal simulation was sampled for a number of MD steps varying from 4000 to 8000 depending on the thermal behaviour of the cluster. At low temperatures, where the clusters remain in their initial configurations, and at high temperatures where melting is obvious, the simulations are performed for 4000 steps (10 picoseconds (ps)). At the intermediate temperatures, where atomic diffusion and structure isomerization take place, the simulations are performed for 8000 steps (20 ps). In each case, three MD simulations were performed to build up reasonable statistics, with the initial temperature varied by 5 K in each series, to ensure that the initial velocities, and therefore the overall trajectories, were different in each of the three series. Hence the thermal behaviour of the clusters was monitored for a total time of 60 ps at the intermediate temperatures. In addition to the three series of 10 and 20 ps simulations, single simulations of 40, 60 and 80 ps were also performed on the Au_7, Au_{13} and Au_{20} tetrahedron, at low and intermediate temperatures. These long simulations were carried out to ensure that the shorter 10 and 20 ps runs were long enough to give unbiased thermal behaviours.

Our simulation times are comparable to the duration of single *ab initio* MD simulations carried out in recent investigations by Chuang *et al* [10] where small Sn clusters were studied for timescales up to 28.8 ps, and Chacko *et al* [11] where Ga clusters were studied using 75 ps simulations. Larger clusters can require longer simulation times particularly near melting points if the melting temperature is to be determined with reasonable statistical accuracy; Chacko *et al* [39] use simulation times of 90 ps at lower temperatures, but up 350 ps near melting points for larger Na clusters. The emphasis of the present work is to investigate the overall melting dynamics at the atomistic scale and relate this to the potential energy surface rather than determine melting temperatures to strict statistical accuracy. By comparing our simulations at selected temperatures run over short versus longer times it is clear that even longer runs would not change the observed overall melting behaviour. In this respect the simulations are sufficiently converged. Melting temperatures deduced from the present simulations, however, are more limited in their statistical significance. Even for times as long as 350 ps there is evidence that the simulations of large Na clusters have still not converged near melting points [39].

The thermal behaviour of the clusters was characterized quantitatively using three different parameters: the root-mean-square bond-length fluctuation δ, the running average of the gradient of δ with respect to simulation time, and the total energy of the cluster. The root-mean-square bond-length fluctuation is defined as

$$\delta = \frac{2}{n(n-1)} \sum_{i<j} \frac{(\langle r_{ij}^2 \rangle_t - \langle r_{ij} \rangle_t^2)^{1/2}}{\langle r_{ij} \rangle_t} \tag{2}$$

where n is the number of atoms in the cluster, r_{ij} is the distance between ions i and j, and $\langle \ldots \rangle_t$ denotes a time average over the trajectory. δ is computed at every step of the simulation and its final value, averaged over the three series, is plotted as a function of the temperature. For bulk systems, the δ versus temperature curve exhibits a clear discontinuity that illustrates a phase transition between solid and liquid. However, for finite-sized systems, the thermal behaviour may be more complex, with the cluster going through a range of structural isomers and other atomic rearrangements. A sharp transition is often not observed in the bond-length fluctuation averaged over the entire MD run.

For this reason is it also useful to extract information of how the bond-length fluctuates over the course of the MD run. To do this we have computed the running average of the

gradient of δ versus MD time step at each temperature:

$$\langle \mathrm{d}\delta \rangle = \left\langle \frac{\mathrm{d}\delta}{\mathrm{d}S} \right\rangle_t \tag{3}$$

where $\mathrm{d}S$ is a 10 MD step interval. The computation of $\langle \mathrm{d}\delta \rangle$ was initiated at 500 steps (1.25 ps) in order to exclude the temperature equilibration process that gives rise to an instantaneous increase of δ. This equilibration time is comparable to that of other recent studies [10, 11] and was arrived at based upon the behaviour of δ. The value of $\langle \mathrm{d}\delta \rangle$, averaged over the three series, is plotted as a function of the temperature. The gradient extracted in this way is not simply the slope of the above bond fluctuation versus temperature curve. It is the time-averaged gradient of δ at each temperature rather than the gradient of the time-averaged δ. It is important to stress that $\langle \mathrm{d}\delta \rangle$ should not be used as an independent criterion but as a complement of the δ versus temperature curve from which it is derived.

Finally, we also report the total energy of each cluster, averaged over the three series, as a function of temperature. This energy is computed as the sum of the electronic potential energy and the ionic kinetic energy of the clusters. The caloric curve is another traditional indicator used to probe the thermal behaviour of a system. As for δ, the total energy of bulk system is expected to show a discontinuity that indicates a solid–liquid phase transition. A smoother caloric curve, on the other hand, suggests a more continuous transition between the solid and liquid phases.

The three parameters described above provide a convenient and logical way to represent the large amount of data generated during the MD simulations. In a sense they are the relevant thermodynamic quantities to examine, although, as Kanhere and co-workers suggest, based upon the analysis of their *ab initio* MD simulations on Na, Sn and Ga clusters [8, 9, 11], the MH technique may be a more complete approach. However, the raw data, and in particular the atomic trajectories during the simulation, provide a qualitative microscopic view of the various thermal processes taking place and allow us to identify structural isomers and melting transitions. This data set is, however, very large and therefore cannot be examined in detail across all the simulations easily.

Simulations for the Au_7 bipyramid were performed for 8000 steps with a 100 K increment between 300 and 1300 K, and a 200 K increment between 1300 and 1900 K. Similarly, simulations for the planar Au_7 structure were performed for 8000 steps. A 200 K increment was used for 300 K $\leqslant T \leqslant$ 1100 K and 1700 K $\leqslant T \leqslant$ 2100 K. In between these two temperature ranges, simulations were performed every 100 K. The Au_{13} ground-state structure MD simulations were performed for 4000 MD steps at 200, 1300, 1500, 1700 and 1900 K. Between 300 and 1100 K, the simulations were performed for 8000 MD steps with a 100 K increment. The Au_{13} icosahedron MD simulations were performed for 4000 MD steps at 100, 1100, 1300, 1500, 1700 and 1900 K. Between 300 and 900 K, the simulations were performed for 8000 MD steps with a 100 K increment. Simulations for the Au_{20} tetrahedron were performed for 4000 steps at 300, 600, 900, 1700, 1800, 2000 and 2200 K. Between 1000 and 1600 K, the simulations were performed for 8000 steps with a 100 K increment. The Au_{20} disordered structure simulations were finally performed for 4000 steps at 300, 400, 1500, 1700 and 1900 K. Between 500 and 1300 K, the simulations were performed for 8000 steps with a 100 K increment. The temperature increments used in these simulations were chosen based upon the thermal behaviour of the cluster. Across the range of temperatures where the clusters exhibit the same behaviour (i.e. remain either in a solid- or liquid-like phase), an increment of 200 K was used. In the temperature ranges where the clusters undergo atomic migration and isomerization processes, the simulations were performed every 100 K.

3. Results

3.1. Au_7

We have previously shown [24] that the planar-to-3D transition in gold clusters occurs at 7 atoms, with the 3D bipyramid being the global minimum and the planar structure a low lying isomer.

The root-mean square bond-length fluctuation, averaged gradient of bond-length fluctuation and caloric curves as a function of simulation temperature are shown in figure 1 for the bipyramid structure. The bond-length fluctuation in figure 1(a) suggests three distinct regions. There appears to be a discontinuity in the slope around 700 K and a change in slope around 1200 K. It is tempting to assign the first of these to a phase transition, which in the bulk material would be interpreted as melting. The averaged gradient shown in figure 1(b) mirrors the above features. It must be stressed that figure 1(b) is not simply the differential of figure 1(a); it is the time-averaged gradient. There are two regions where the gradient does not change significantly, one where the gradient is relatively small up to 600 K and one with large gradient above about 1200 K. The discontinuity in the bond-length curve at 700 K is reflected by an increase in the gradient curve at 700 K. The intermediate region is more interesting, where the gradient more than doubles between 700 and 1200 K. Obviously this is a manifestation of the way the bond-length changes over time at a given temperature, or equivalently the dynamic behaviour of the atoms during a simulation. Below 600 K, the isothermal δ versus MD step curves (not reported in the present communication) are relatively flat and the averaged gradient is therefore small. Between 700 and 900 K, there are discrete steps in the isothermal δ curve that result in the final value of δ being considerably higher at 700 K than at 600 K. However, this step increase affects only moderately the overall $\langle \mathrm{d}\delta \rangle$ value due to the localized nature of the increase. Above 900 K, δ is found to increase monotonically, which results in the sharp increase in $\langle \mathrm{d}\delta \rangle$.

The total energy, figure 1(c), as a function of the temperature is relatively structureless, increasing at a relatively constant rate with increasing temperature. This would be more indicative of a continuous transition between the solid- and liquid-like phases.

Examination of the MD trajectories revealed that, below 700 K, the positions of the atoms remain the same with respect to each other. The atoms simply vibrate about their equilibrium position with relatively low amplitude; the cluster is in a solid-like phase. At higher temperatures, the bipyramid structure undergoes structural transformations whose frequency increases with temperature. Between 700 and 900 K the MD trajectories show specific transitions taking place between the bipyramid and three other structures: a C_{4v} triangular structure (see II in figure 2), a one-atom capped octahedron (see III in figure 2) and a three-atom capped tetrahedron (see IV in figure 2), respectively. In the timescale of the simulations, these structures are found to be stable, i.e. observed for more than 1 ps, and are therefore considered as structural isomers. As shown in figure 2, these isomers are almost energetically equivalent but lie more than 0.02 eV/atom higher in energy than the bipyramid structure. Above 900 K, the structural isomerization processes still take place but coexist with geometrical transformations between 'amorphous' structures that do not exhibit any symmetry. Beyond 1100 K, these amorphous structural transitions are found to be strongly predominant and occur at an increasingly high frequency; this is a region of liquid-like behaviour.

Figure 3 shows the results of the simulations for the planar structure. The bond-length fluctuation and gradient curves indicate a different thermal behaviour compared with the 3D bipyramid structure. Both curves contain two regions with different slope, and a transition occurring around 900 K. They also show similar oscillations above 1000 K. This variation is

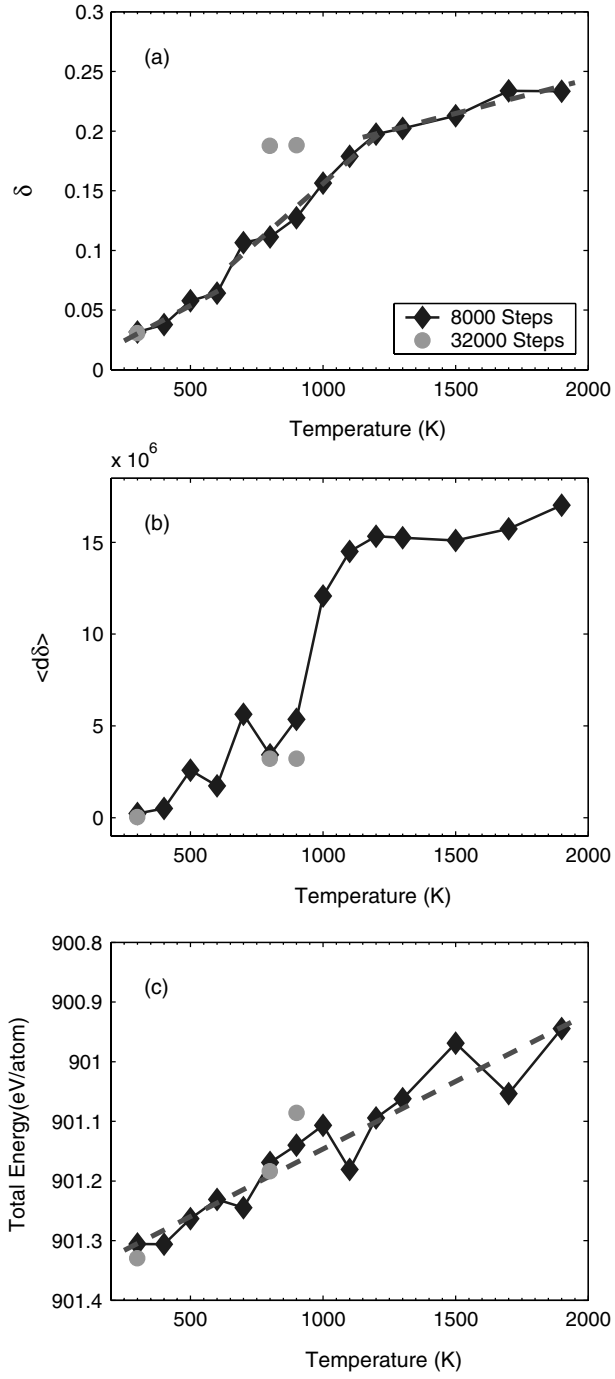

Figure 1. Au_7 bipyramid bond-length fluctuation δ (a), time-averaged gradient of bond-length fluctuation $\langle d\delta \rangle$ (b) and total energy (c) as a function of temperature.

due to the non-uniformity of our data, which results in a relatively poor statistical average. For instance, at a given temperature above 900 K, δ is found to remain constant with relatively low values in two series while in contrast it increases monotonically in the third one, and vice versa at the next temperature. The total energy of the planar structure shows the same overall

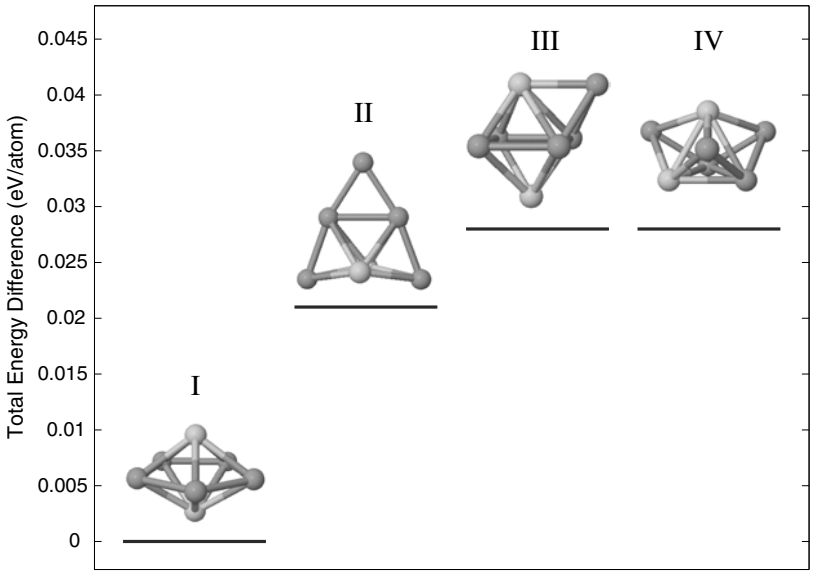

Figure 2. Structural isomers of Au_7 lying close in energy to the bipyramid structure.

behaviour as the bipyramid structure, increasing linearly as a function of the temperature as shown in figure 3(c) even though both structures have a considerably different thermal behaviour.

The atomic trajectories reveal that the planar structure remains in a solid-like phase with the atoms vibrating around their equilibrium positions, up to 900 K. Migration of the atoms within the structure occurs at around 1100 K, although even at this temperature the structure has not entered a liquid-like phase. Between 1100 and 1600 K, the thermal behaviour of the Au_7 planar structure is dominated by the two sets of structural transformations reported in figure 4. The first transformation is from the one-atom capped triangle to the three-atom capped square then back again, figure 4(a). Although not altering the original structure, this transformation results in a change of atomic configuration and therefore an increase in δ and $\langle d\delta \rangle$ due to the difference in second- and third-nearest neighbour distances. The second structural transformation, figure 4(b), is a 90° rotation of atoms 1 and 2 perpendicular to the plane of the structure. This transformation results in a stable 3D structure (see IV in figure 4(b)) that is 0.016 eV/atom higher in energy than the planar structure. However, due to thermal energy, this structure undergoes further structural degeneration with the bond between atoms 1 and 2 alternating between a $\pm 30°$ rotation around the bond formed by atoms 3 and 4 (see V in figure 4(b)). Beyond 1600 K, the thermal behaviour of the planar structure is similar to the bipyramid whereby the above structural transformations are found to coexist with amorphous structural transitions that become more dominant as the temperature increases.

The results of the 80 ps simulations of the bipyramidal and planar structures are consistent with the results extracted from the shorter simulations (see figures 1 and 3). The atomic trajectories follow the same isomerization and atomic rearrangement processes as those described above and illustrated in figures 2 and 4. In the case of the bipyramid, at 800 and 900 K, δ increases considerably from 8000 to 32 000 steps due to the increase in the total number of structural isomerizations taking place in 80 ps (see figure 1). The total energies of the structures resulting from these long simulations are found to be close to the corresponding averaged values of the shorter runs as shown in figures 1(c) and 3(c). These results give us

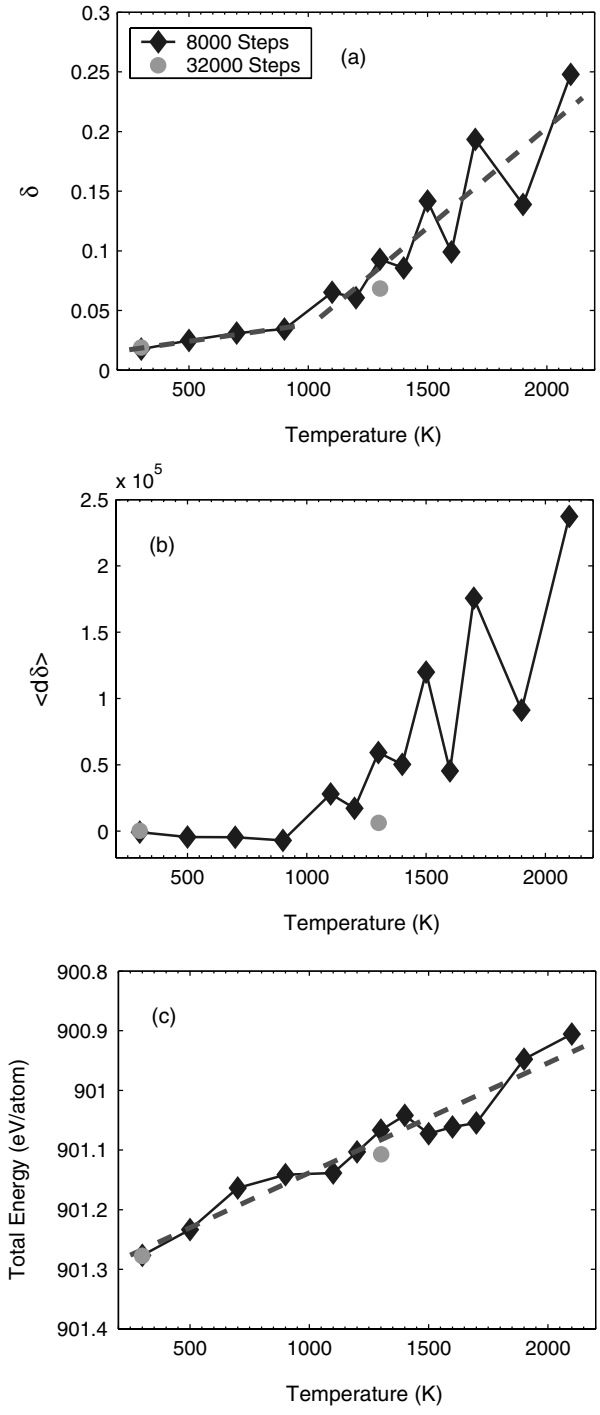

Figure 3. Au_7 planar structure bond-length fluctuation δ (a), time-averaged gradient of bond-length fluctuation $\langle d\delta \rangle$ (b) and total energy (c) as a function of temperature.

confidence that our simulations, although not yielding fully converged bond-length fluctuations curves at all temperatures, are long enough to provide a qualitatively accurate representation of the steady-state/thermally equilibrated behaviour of the clusters.

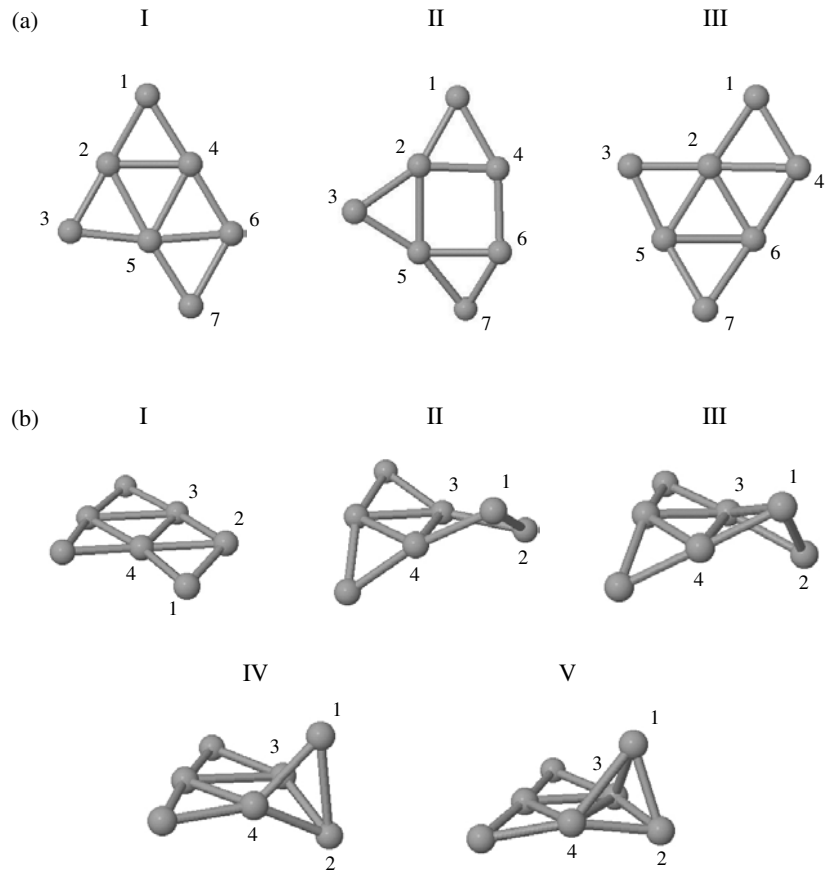

Figure 4. Au_7 planar structure atomic rearrangement (a) and isomerization process (b).

3.2. Au_{13}

The ground-state structure and icosahedron [24] were used as the starting points for the 13-atom simulations. The results for the ground-state structure are shown in figure 5. The bond-length fluctuation and caloric curves have a similar form, showing a near linear increase with temperature. The time-averaged gradient on the other hand exhibits a discontinuity between 1100 and 1300 K. As in the case of the Au_7 bipyramid, this discontinuity results from a step-like increase of δ between 400 and 1100 K that contrasts with a more gradual increase occurring beyond this temperature range.

The atomic trajectories reveal that, below 400 K, the atoms vibrate about their mean positions leaving the structure in its original configuration, in a solid-like phase. Between 400 and 1100 K, the Au_{13} ground-state structure undergoes specific structural transformations, which results in the cluster passing among four main isomers as shown in figure 6: a C_{4v} structure labelled III and two C_{2v} structures labelled II and IV. These isomers all lie within 0.01 eV/atom of the ground-state structure. Beyond 1100 K, these isomerization processes tend to disappear and be replaced by structural transition between amorphous structures consistent with a liquid-like behaviour. Consequently, non-symmetrical structures are mainly observed after 4000 steps at 1300 K and above.

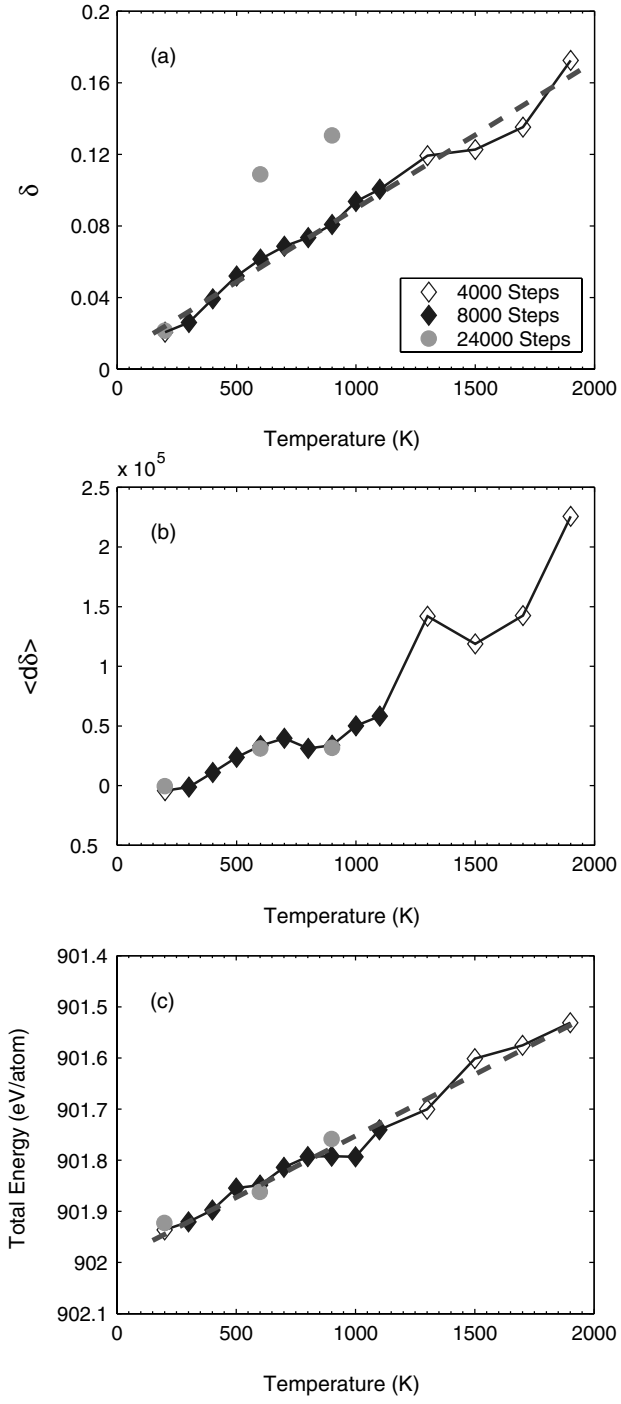

Figure 5. Au_{13} ground-state structure bond-length fluctuation δ (a), time-averaged gradient of bond-length fluctuation $\langle d\delta \rangle$ (b) and total energy (c) as a function of temperature.

Above 300 K the corresponding curves, figure 7, for the icosahedral 13-atom structure are similar to the ground-state structure. At a temperature of 300 K and below, the time-averaged gradient in figure 7(b) is negative, indicating that, after the initial equilibration, δ

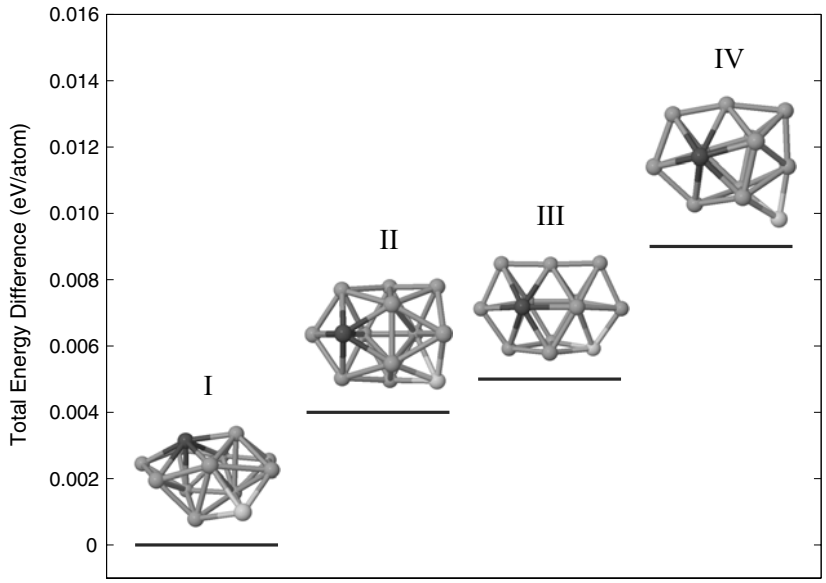

Figure 6. Structural isomers of Au_{13} lying close in energy to the ground-state structure.

slowly decreases during the course of the simulation. In addition there is a sharp rise in the time-averaged gradient around 1100 K. In analogy with the Au_7 and Au_{13} ground-state structures, this discontinuity is not observed in the bond-length fluctuation and accounts for the transition between the step-like and gradual increase of δ taking place around 1100 K.

The MD trajectories show that the icosahedral structure is highly unfavourable. Even at the lowest temperature, the cluster transforms to the cuboctahedral structure (see II in figure 8) within the first 500 steps of thermal equilibration. As expected, the cuboctahedron is found to be lower in energy than the icosahedron, by 0.037 eV/atom, but still significantly higher than the Au_{13} ground-state structure (see figure 8). Once formed, the cuboctahedron remains stable up to 300 K. Between 400 and 900 K, the cluster undergoes the same structural transformations as those reported for the Au_{13} ground-state structure between 400 and 1100 K. In this temperature range, the structure therefore goes through the different isomers shown in figure 6. Above 900 K, these isomerization processes are found to become less significant, to the benefit of transitions between amorphous structures. As the temperature increases, the structure becomes liquid-like.

In view of the thermal behaviour reported above, it is therefore not surprising that the Au_{13} icosahedron exhibits a linear caloric curve identical to that of the Au_{13} ground-state structure except for $T \leqslant 300$ K. As mentioned above, below 400 K, the Au_{13} is in a cuboctahedral structure whose potential energy is unfavourable with respect to the global minima

As in the case of Au_7, the 60 ps simulations yield results that are consistent with those of the shorter simulations both quantitatively and qualitatively. With the exception of the δ value of the Au_{13} ground-state structure at 600 and 900 K, the longer simulations yield bond-length fluctuations and total energies that are similar to the 10 and 20 ps averaged values. The increase in δ for the Au_{13} ground-state structure at 600 and 900 K is due to an increase in the total number of structural isomerizations taking place in 60 ps, as previously observed for the Au_7 bipyramid. The atomic trajectories of these long simulations finally report the same isomerization processes as those observed in the shorter runs across the entire 60 ps.

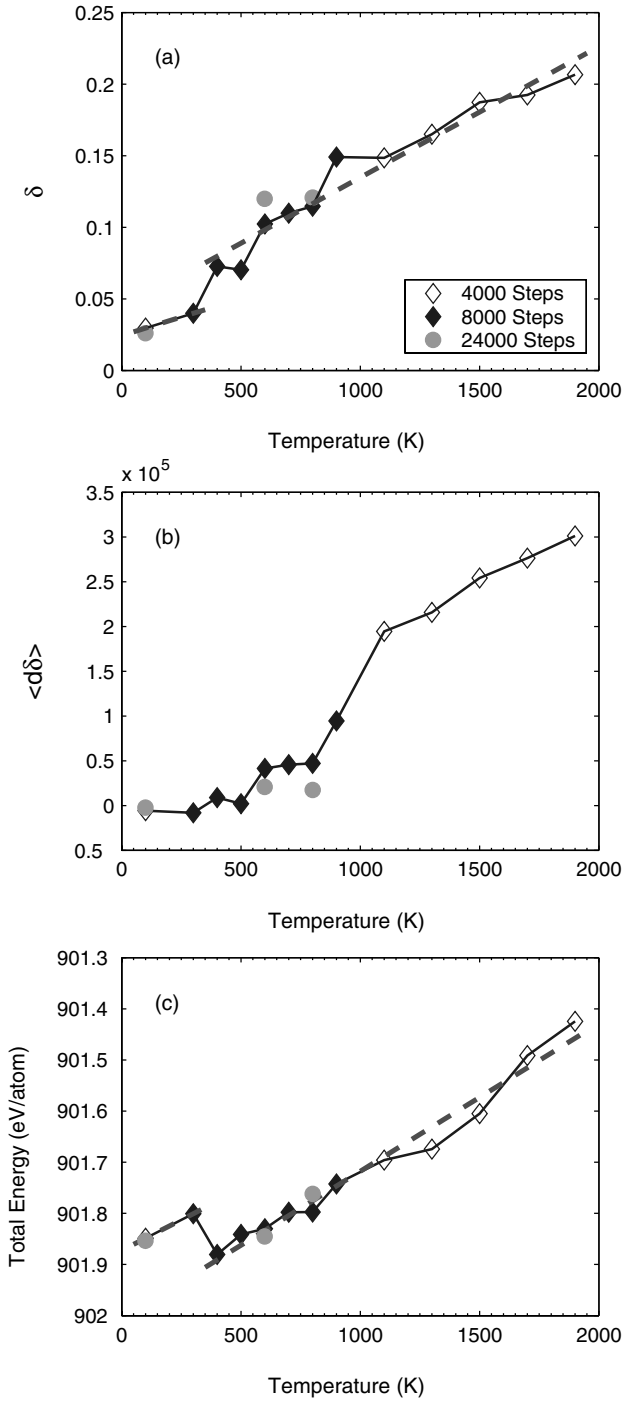

Figure 7. Au_{13} icosahedron bond-length fluctuation δ (a), time-averaged gradient of bond-length fluctuation $\langle d\delta \rangle$ (b) and total energy (c) as a function of temperature.

3.3. Au_{20}

Surprisingly, the highly symmetric tetrahedron structure is the global minimum for the 20-atom cluster. The atoms in this cluster are arranged in the bulk fcc structure with only a

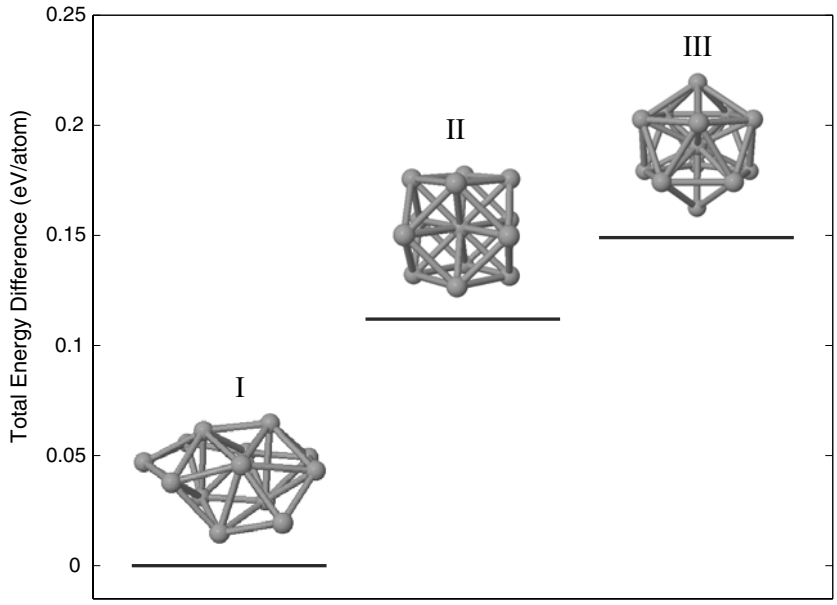

Figure 8. Structural isomers of Au_{13} lying close in energy to the icosahedron structure.

slight distortion [24]. The results of the 10 and 20 ps simulations, as shown in figure 9, can be interpreted as showing that there is a relatively sharp transition between two structures at about 1400 K. This suggests that the tetrahedron shows a clear transition between solid-like and liquid-like phases. The MD trajectories support this interpretation. Between 1400 and 1600 K, the distortions become very large and eventually result in the migration of a corner atom, which triggers the melting of the cluster. At 1700 K and above, the atomic migration occurs during the temperature equilibration, leaving the cluster to go through a series of amorphous structural transitions for the rest of the simulations. The situation at 1200 K is less clear cut, with the tetrahedron maintaining its original configuration in the 10 and 20 ps simulations, but melting in the 40 ps simulation (figure 9(c)). However, in this longer simulation, the atomic trajectory reveals that the melting behaviour is identical to that described in the shorter simulations, and the cluster does not undergo structural isomerization prior to melting. In addition this melting is found to occur within the first 2000 MD steps of the longest simulation. Hence it is not the length of the simulation that affects the results, but rather the initial conditions (i.e. initial velocities).

This melting behaviour is not so clear if a low-lying disordered isomer is used as the starting point for the simulation. The resulting bond-fluctuation, averaged gradient and caloric curves are given in figure 10. There is an indication of a discontinuity in the bond-length fluctuation at about 700 K, but this is not reflected in the other two curves. The atomic trajectories reveal that at low temperature, i.e. below 700 K, the cluster undergoes a structural transformation but remains in a solid-like phase. These atomic rearrangements are observed at a temperature as low as 300 K, in the initial temperature equilibration as well as in the rest of the simulation. The various structures associated with the 20-atom cluster are shown in figure 11. Between 300 and 600 K, the disordered structure (labelled IV in figure 11) is found to coexist with two main isomers: a disordered structure labelled II and a C_{4v} structure labelled III (see figure 11). As reported in figure 11, these two isomers are more favorable than the initial structure but

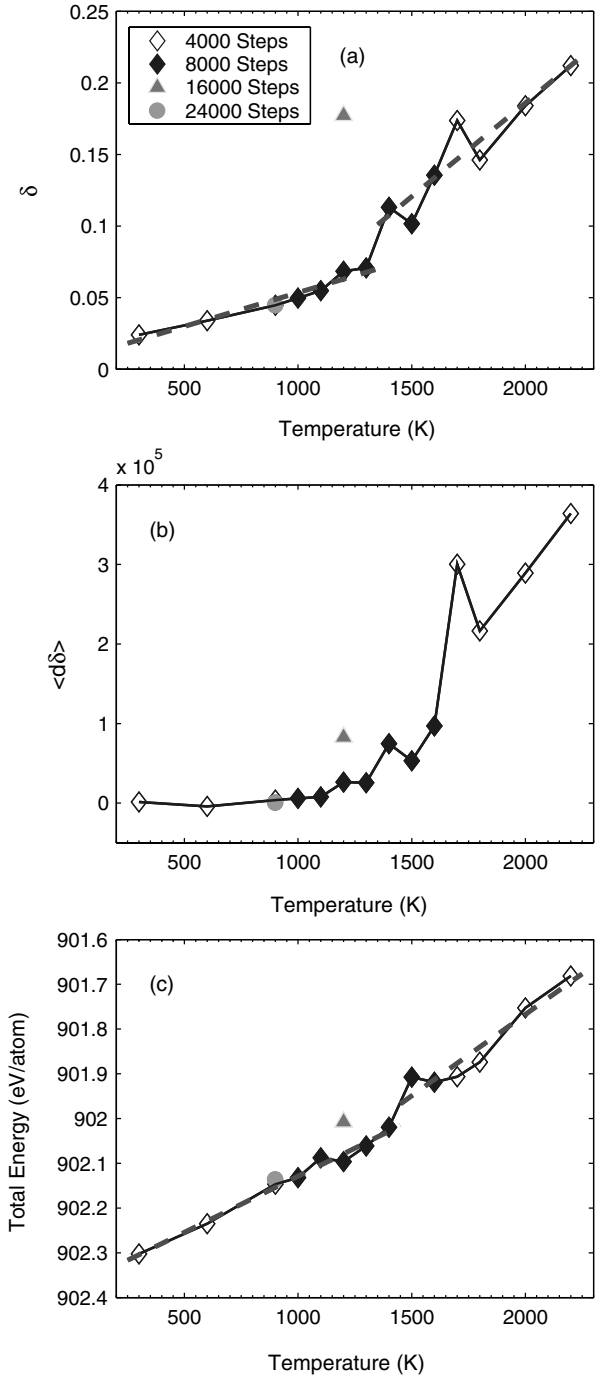

Figure 9. Au_{20} tetrahedron bond-length fluctuation δ (a), time-averaged gradient of bond-length fluctuation $\langle d\delta \rangle$ (b) and total energy (c) as a function of temperature.

lie more than 0.015 eV/atom higher in energy than the tetrahedron. Above 600 K, the cluster exhibits a liquid-like behaviour, going through a series of amorphous structural transitions that result in final geometries that are non-symmetric for $T \geqslant 700$ K.

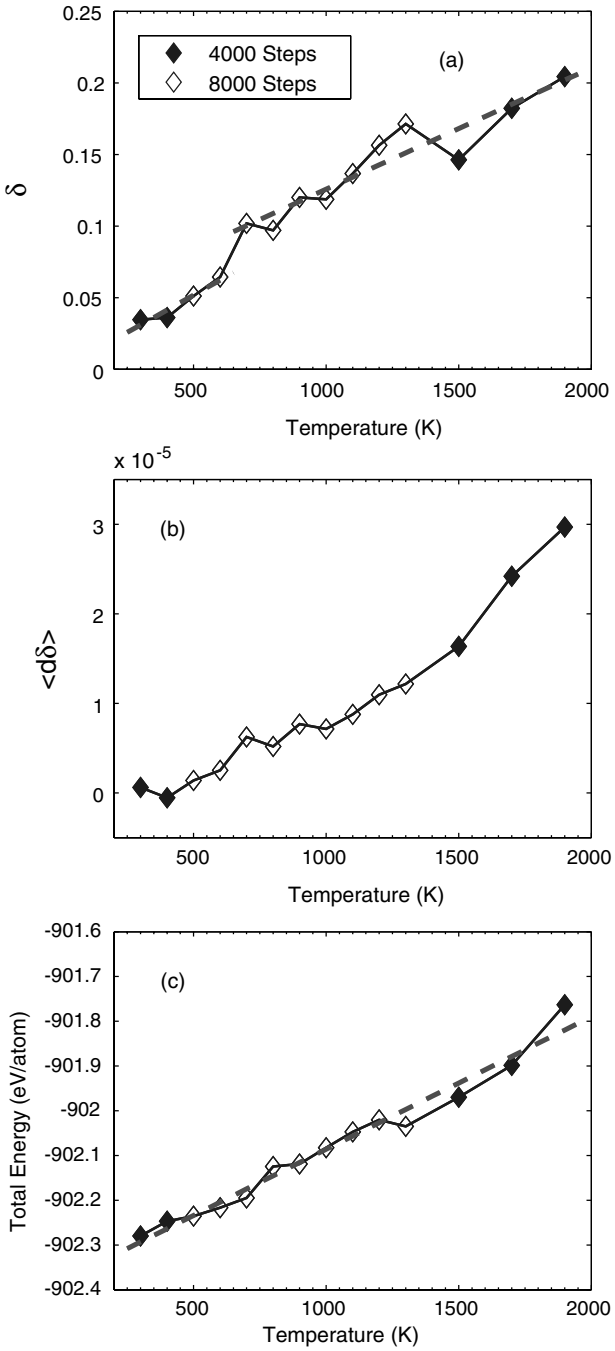

Figure 10. Au_{20} disordered structure bond-length fluctuation δ (a), time-averaged gradient of bond-length fluctuation $\langle d\delta \rangle$ (b) and total energy (c) as a function of temperature.

4. Discussion

The thermal behaviour of the Au_7 bipyramid is different to the behaviour of the planar structure both quantitatively and qualitatively. The bipyramid undergoes structural transformations at 700 K before becoming liquid-like at 1100 K. By contrast the planar triangle-based structure

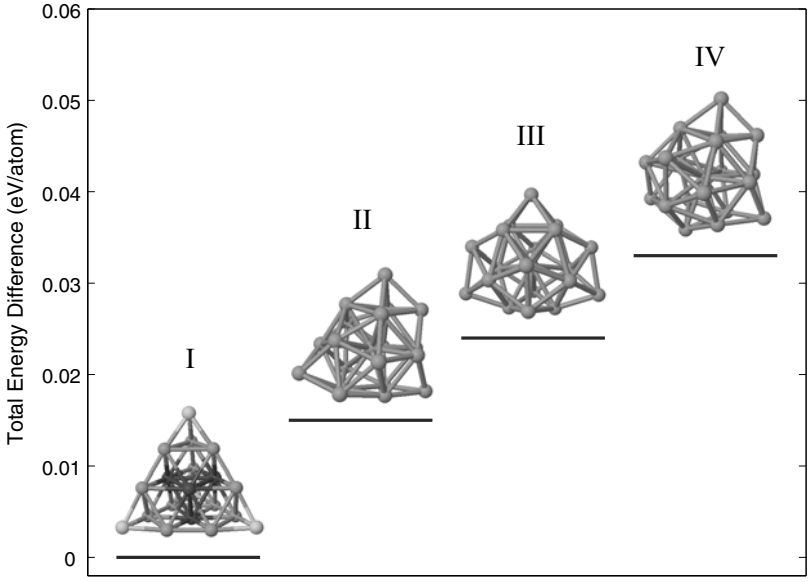

Figure 11. Au_{20} structural isomers.

is found to remain in its initial atomic configuration up to 900 K and to retain the same geometry up to 1600 K. The bipyramid undergoes three distinct isomerization processes in the transition regime between solid- and liquid-like phases whereas the planar structure is found to coexist with a single close-lying isomer before melting. This difference in thermal behaviour may indicate that the bipyramid and the planar structure belong to distinct portions of the potential energy surface (PES). Or equivalently, it may indicate that the MD simulations do not consistently sample both regions of the PES in a single run, even at temperatures well above the melting point. The PES in the region of the minimum for the bipyramid can be compared to the 'heavily-worn staircase' as referred to by Berry [17]; the PES is expected to consist of a succession of potential wells associated with each structural isomer separated by relatively low energy barriers. These energy barriers correspond to an atom in the pentagonal ring (coloured in dark grey in I figure 2) moving in a direction perpendicular to the plane formed by the four remaining atoms. This atomic migration transforms the bipyramid structure into the capped octahedral and the tri-capped tetrahedral structures (see III and IV in figure 2). The C_{4v} structure, labelled II in figure 2, is obtained by a capping atom of the tetrahedral structure rotating by an angle of 60°.

The thermal behaviour of these small clusters can also be considered from a 'molecular' viewpoint, which is through the concepts of bond energies and vibrational frequencies. Contrary to what is expected from their nearest-neighbour coordination, the pentagonal ring atoms are found to have a bond energy 0.575 eV lower than that of the top/bottom atoms. Additionally, for the lowest frequency vibrational modes at 50.6, 52.0 and 52.6 cm^{-1}, the pentagonal ring atoms are found to vibrate with the largest amplitudes in directions nearly perpendicular to the ring plane, while the top and bottom atoms oscillate with a small amplitude in a direction parallel to the pentagonal ring.

The melting behaviour of the planar structure shows that the PES in this region consists of a deep minimum with a single additional well corresponding to the 3D isomer (see IV in figure 4(b)) located on the side of this well.

The Au_7 bipyramid undergoes a continuous transition from solid- to liquid-like phase going through a series of isomerization processes. The planar structure on the other hand undergoes a single isomerization process along with an atomic rearrangement (see figure 4) prior to becoming liquid-like.

The two 13-atom structures investigated show similar thermal behaviour, which is perhaps surprising given that one structure is disordered (the global minimum) and the other is an ordered icosahedron. Both clusters undergo identical structure isomerizations above 300 K. The local minimum in the PES associated with the icosahedral structure must be shallow with a slightly deeper minimum associated with the cuboctahedral structure located close by. This is easily inferred from the rapid transformation from icosahedral to cuboctahedral at low temperatures. In the vicinity of the global minimum, similar to Au_7, the Au_{13} PES is expected to have several small wells corresponding to the observed isomers which results in the cluster having a continuous transition between solid- and liquid-like phases. The different isomerizations of the ground-state structure take place via coordinated atomic rearrangements.

The atomic binding energies are found to increase gradually from the weakest-bonded atom, being the octahedron capping atom (coloured in light grey in I figure 6), to the strongest-bonded atom, being the pentagonal ring top capping atom (coloured in dark grey in I figure 6). The difference in binding energy between these two atoms is 0.542 eV. The vibrational analysis reveals that for low-frequency modes most of the atoms vibrate with similar amplitude in directions nearly perpendicular to the plane formed by the interpenetrating octahedron and pentagonal bipyramid. Unlike the Au_7 ground-state structure, whose atoms have very distinct vibrational and energetic properties, the Au_{13} ground-state structure appears to be more uniform. This is consistent with the isomerization processes occurring.

In contrast to the present study, Garzón and Jellinek [40] and Rey *et al* [19] reported caloric curves for the Au_{13} icosahedron that exhibited a sharp discontinuity, suggesting a bulk-like thermal behaviour with a relatively well-defined transition between solid- and liquid-like phases. The tight-biding (TBM) potentials used in these studies predict a melting temperature of 413 [19] and 680 K [40], that is considerably lower than the temperature at which we report the Au_{13} becoming liquid-like, but comparable to the temperature at which the ground-state structure and the cuboctahedron isomerize. These semi-empirical studies suggest that the TBM semi-empirical potentials generate a PES with a deep well centred on the icosahedral structure, and that the TBM potential tends to favour highly coordinated structures over more open or disordered structures.

The two 20-atom clusters also exhibit very distinct thermal behaviours. While the disordered structure is found to isomerize at low temperatures before becoming liquid-like at 700 K, the tetrahedron is on the other hand found to remain in its initial atomic configuration until it melts at about 1200 K. Unlike all the other structures studied, the Au_{20} tetrahedron does not undergo any structural isomerization prior to melting. The thermal behaviour of the ground-state structure, which is consistent with a bulk material, indicates that the tetrahedron sits at the bottom of a deep, isolated energy well.

Melting of the ground-state tetrahedral structure, as observed earlier in the MD trajectories, is triggered by the migration of a corner atom. These corner atoms (coloured in light grey in I figure 11), as expected from their coordination, have the smallest binding energy, 0.552 eV smaller than the edge atoms (coloured in grey in I figure 11) and 0.700 eV smaller than the face centred atoms (coloured in dark grey in I figure 11). The vibrational analysis indicates that for the three lowest vibration modes of 31.6, 34.6 and 36.9 cm^{-1}, the weakly bound corner atoms vibrate with the largest amplitudes.

Finally, given the well-accepted belief that the melting point decreases with decrease in particle size, the finding here that this trend is reversed for exceedingly small clusters may

merit some brief further consideration. As mentioned previously, the trend in decreasing melting point is driven by considerations of increasing ratio of surface area to volume in particles. The decrease is driven by classic and continuum phenomena and is not directly influenced by the internal structure of the material. However, diffraction studies of liquid metals reveals that their atoms certainly possess a degree of very short range clustering and ordering, extending perhaps to nearest and next-nearest neighbours [41–43]. These transient clusters, consisting of a dozen or so atoms, persist to temperatures considerably above the melting point of the bulk material, and appear to have structures related to those of the corresponding solid material. For example, they are fcc in nature in fcc metals [42] and bcc in nature in bcc metals [43]. Our discrete clusters are roughly of the same size as those that form transiently in the liquid state. We propose that the trend of decreasing melting point with size is reversed when this situation is attained because the low viscosity and macroscopic atomic disorder of the bulk liquid state in metals can no longer be established.

5. Conclusion

The present investigation supports previous experimental and theoretical studies on tin [4, 9, 10] and gallium [5, 11] clusters, which suggest an increase in melting temperature as the cluster size is reduced to less than 50 atoms. By contrast, for gold, experiments down to 20 Å diameter clusters [1] and semi-empirical simulations down to 10 Å diameter [6, 14–16] clusters report a melting temperature that decreases as 1/diameter. The present study reports melting temperatures, i.e. temperatures at which the clusters become 'liquid-like', that are in the same range as or above the melting temperature of the bulk metal. For the planar Au_7 cluster, the melting temperature found throughout the simulations exceeds that of the bulk. However, it is important to stress that the present simulations may yield an overestimation of the melting temperatures due to the relatively short total time of the simulation and number of initial conditions explored.

The Au_{20} cluster is particularly interesting because in its ground state, it has an extremely symmetric tetrahedral geometry that is a portion of bulk metal. Unlike all the other clusters studied here it shows a sharp melting transition at a temperature of 1200 K, comparable to the melting point of bulk gold. Unlike all the other structures studied here, it does not undergo any structural isomerization or atomic rearrangement before melting.

The present study shows that for these very small clusters there is no clear correlation between melting temperature and the cluster size, or rather the macroscopic idea of a sharp melting/freezing transition is not easily applied to such small collections of atoms. The clusters, with the exception of Au_{20}, exist in 'slush-like' state [17] over a wide temperature range.

From the molecular perspective the MD simulations are probing the shape of the potential energy surface; clearly, the melting behaviour is determined by the shape of the PES. The results presented here suggest that small gold clusters containing tens of atoms have relatively flat PESs with a large number of minima. The MD simulations sample these minima as a function of temperature, giving rise to structural isomerization over a wide temperature range rather than a well-defined melting point. At sufficiently high temperature the simulation does not remain in any of the minima very long and the cluster appears to melt. Again, Au_{20} is in contrast to this general behaviour. Its defined transition suggests an isolated, relatively deep potential well corresponding to the tetrahedron surrounding by a flat plateau. The cluster remains confined within this well until about 1200 K when it can escape into a region of the PES corresponding to a liquid-like structure.

Acknowledgments

This work was supported by the University of Technology, Sydney (UTS) and the Australian Research Council. Computing facilities were accessed through the merit allocation schemes of the APAC National Facility and AC3 in NSW. B Soulé de Bas acknowledges receipt of an International Postgraduate Research Scholarship and stipend from the Faculty of Science, UTS.

References

[1] Buffat P and Borel J-P 1976 *Phys. Rev.* A **13** 2287
[2] Schmidt M, Kusche R, Kronmüller W, von Issendorff B and Haberland H 1997 *Phys. Rev. Lett.* **79** 99
[3] Schmidt M, Kusche R, von Issendorff B and Haberland H 1998 *Nature* **393** 238
[4] Shvartsburg A A and Jarrold M F 2000 *Phys. Rev. Lett.* **85** 2530
[5] Breaux G A, Benirschke R C, Sugai T, Kinnear B S and Jarrold M F 2003 *Phys. Rev. Lett.* **91** 215508
[6] Cleveland C L, Luedtke W D and Landman U 1999 *Phys. Rev.* B **60** 5065
[7] Rytkönen A, Häkkinen H and Manninem M 1998 *Phys. Rev. Lett.* **80** 3940
[8] Vichare A, Kanhere D G and Blundell S A 2001 *Phys. Rev.* B **64** 045408
[9] Joshi K, Kanhere D G and Blundell S A 2002 *Phys. Rev.* B **66** 155329
[10] Chuang F-C, Wang C Z, Ögüt S, Chelikowsky J R and Ho K M 2004 *Phys. Rev.* B **69** 165408
[11] Chacko S, Joshi K, Kanhere D G and Blundell S A 2004 *Phys. Rev. Lett.* **92** 135506
[12] Koga K, Ikeshoji T and Sugawara K-I 2004 *Phys. Rev. Lett.* **92** 115507
[13] Dick K, Dhanasekaran T, Zhang Z and Meisel D 2002 *J. Am. Chem. Soc.* **124** 2312
[14] Ercolessi F, Andreoni W and Tosatti E 1991 *Phys. Rev. Lett.* **66** 911
[15] Lewis L J, Jensen P and Barrat J-L 1997 *Phys. Rev.* B **56** 2248
[16] Shim J-H, Lee B-J and Cho Y W 2002 *Surf. Sci.* **512** 262
[17] Berry R S 1994 *Springer Ser. Chem. Phys.* **52** 187
[18] Beck T L and Berry R S 1988 *J. Chem. Phys.* **88** 3910
[19] Rey C, Gallego L J, García-Rodeja J, Alonso J A and Iñiguez M P 1993 *Phys. Rev.* B **48** 8253
[20] García-Rodeja J, Rey C, Gallego L J and Alonso J A 1994 *Phys. Rev.* B **49** 8495
[21] Li T X, Ji Y L, Yu S W and Wang G H 2000 *Solid State Commun.* **116** 547
[22] Ferrenberg A M and Swendsen R H 1988 *Phys. Rev. Lett.* **61** 2635
[23] Labastie P and Whetten R L 1990 *Phys. Rev. Lett.* **65** 1567
[24] Soulé de Bas B, Ford M J and Cortie M B 2004 *J. Mol. Struct. THEOCHEM* **686** 193
[25] Hutchings G J 1985 *J. Catal.* **96** 292
[26] Haruta M, Kobayashi T, Sano H and Yamada M 1987 *Chem. Lett.* **2** 405
[27] Li J, Li X, Zhai H-J and Wang L-S 2003 *Science* **299** 864
[28] Sánchez-Portal D, Ordejón P, Artacho E and Soler J M 1997 *Int. J. Quantum Chem.* **65** 453
[29] Soler J M, Artacho E, Gale J D, García A, Junquera J, Ordejón P and Sánchez-Portal D 2002 *J. Phys.: Condens. Matter* **14** 2745
[30] Nosé S 1984 *Mol. Phys.* **52** 255
[31] Perdew J and Zunger A 1981 *Phys. Rev.* B **23** 5075
[32] Pyykkö P 1988 *Chem. Rev.* **88** 563
[33] Häkkinen H, Moseler M and Landman U 2002 *Phys. Rev. Lett.* **89** 033401
[34] Schwerdtfeger P 2002 *Heteroatom Chem.* **13** 578
[35] Fernández E M, Soler J M, Garzón I L and Balbás L C 2005 *Int. J. Quantum Chem.* **101** 740
[36] Troullier N and Martins J L 1991 *Phys. Rev.* B **43** 1993
[37] Artacho E, Gale J D, García A, Junquera J, Martin R M, Ordejón P, Sánchez-Portal D and Soler J M 2003 *User's Guide SIESTA 1.3* (Madrid: Fundación General Universidad Autónoma de Madrid)
[38] Boys S F and Bernardi F 1970 *Mol. Phys.* **19** 553
[39] Chacko S, Kanhere D G and Blundell S A 2005 *Phys. Rev.* B **71** 155407
[40] Garzón I L and Jellinek J 1991 *Z. Phys.* D **20** 235
[41] Ilinskii A, Kaban I, Koval Y, Hoyer W and Slyusarenko S 2004 *J. Non-Cryst. Solids* **345/346** 251
[42] Roik A S, Kazimirov V P and Sokolskii V E 2004 *J. Struct. Chem.* **45** 648
[43] Pan X M, Bian X F, Qin J Y and Wang W M 2002 *Mater. Sci. Technol.* **18** 1301